CORA Cork Open Research Archive
Cartlann Taighde Oscailte Chorcaí

Title	Characterisation of the electroless nickel deposit as a barrier layer/under bump metallurgy on IC metallisation
Authors	Rohan, James F.;O'Riordan, Gerard
Publication date	2002-11-07
Original Citation	Rohan, J. F. and O'Riordan, G. (2003) 'Characterisation of the electroless nickel deposit as a barrier layer/under bump metallurgy on IC metallisation', Microelectronic Engineering, 65(1), pp. 77-85. doi: 10.1016/S0167-9317(02)00730-X
Type of publication	Article (peer-reviewed)
Link to publisher's version	http://www.sciencedirect.com/science/article/pii/S016793170200730X - 10.1016/S0167-9317(02)00730-X
Rights	© 2003 Elsevier B.V. All rights reserved. This manuscript version is made available under the CC-BY-NC-ND 4.0 license - http://creativecommons.org/licenses/by-nc-nd/4.0/
Download date	2025-04-29 01:04:10
Item downloaded from	https://hdl.handle.net/10468/7622

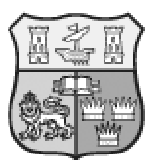
UCC
University College Cork, Ireland
Coláiste na hOllscoile Corcaigh

Characterisation of the electroless nickel deposit as a barrier layer /under bump metallurgy on IC metallisation

James F. Rohan*, Gerald O'Riordan

National Microelectronics Research Centre, Lee Maltings, Prospect Row, Cork, Ireland

Abstract

Selective electroless nickel–phosphorus deposits on integrated circuit (IC) metallisation such as copper and aluminium were characterised using differential scanning calorimetry (DSC), X-ray diffraction (XRD), scanning electron microscopy (SEM) and energy dispersive X-ray (EDX) for elemental analysis. Annealing the Ni–P deposits in nitrogen atmospheres at temperatures compatible with organic dielectrics for IC components, such as polyimide, was performed to characterise the deposits. The crystallisation behaviour of the electroless nickel deposits with different concentrations of co-deposited phosphorus was examined.

Keywords: Electroless; IC metallisation; Barrier; Crystallisation

1. Introduction

Electroless nickel may be utilised as a barrier layer material [1], wirebond substrate [2] or an under bump metallurgy on the I/O bond pads of integrated circuits (IC's) [3]. Thicker deposits may function as chip bumps, for example, when used in collaboration with anisotropically conductive adhesives The adhesion of electroless nickel deposits has been found to increase significantly when annealed at temperatures of 300 to 400 °C [4].This temperature range is of significance for the IC industry as it represents the maximum temperature to which the commonly used dielectric, polyimide, may be subjected in the cured state without degrading. Characterisation of the electroless nickel deposit during such temperature processing on IC level substrates will assist in understanding the capabilities of this system as a barrier/bonding layer material for low cost processing of current and future IC's.

A selective electroless process for the deposition of barrier/bonding layer materials would greatly

reduce costs. Electroless nickel protection of copper is common in PCB manufacturing. Electroless nickel–phosphorus has been reported to be significantly more effective than electroplated nickel in preventing copper diffusion [5]. The authors also state that barrier properties of electroless nickel improve with increased nickel layer thickness and phosphorus content with 8–10% phosphorus content the most effective barrier to Cu/Au interdiffusion. Thicker barrier layer materials may be used on the final metallisation of the I/O bond pad than is permitted to protect the via and line metallisation of the IC. For this reason electroless nickel may be sufficient to function as a barrier layer material.

The substantially amorphous nature of the as-plated electroless nickel/phosphorus deposit has been determined by powder X-ray diffraction (PXRD) [7,10,12]. Graham et al. [6] have described the deposited Ni–P alloy as a supersaturated solid solution of phosphorus dissolved in crystalline nickel. They also suggest that the crystallinity of Ni–P alloys with less than 7 w/o phosphorus is supported by the appearance of eight to 11 reflections in their diffraction patterns. As little as 2 v/o (volume per cent) of Ni_3P may produce lines in the electron transmission diffraction patterns. A deposit with 7 w/o phosphorus, for example, would contain 50 v/o of Ni_3P if the phosphorus were all combined with the nickel in the form of the compound. When Ni–P is heat treated to about 400 °C, crystallinity increases to 75%. Beyond this temperature, the improvement in crystallinity is not very high, reaching about 86% at 600 °C [7]. The crystalline material upon heat treatment of nickel phosphorus deposits has been attributed to Ni and Ni_3P phases [7,10].

2. Experimental

The substrates for the electroless nickel deposition were sputtered copper (5000 Å) on titanium (2000 Å) on 1000 Å thermally grown SiO_2 on 4″ silicon wafers. The metals were deposited using a Nordiko DC Magnetron sputterer. Electroless deposits were analysed by scanning electron microscopy (SEM) using a Hitachi S-4000 Field effect SEM with a PGT IMIX energy dispersive X-ray (EDX) system with intensity correction for elemental analysis The phosphorus content was determined by EDX analysis. The hypophosphite based electroless nickel baths comprising nickel sulphate, hypophosphite and calcium succinate were operated at a pH value of between 4.6 and 6.0 at temperatures of 85–95 °C. Varying the plating bath pH and solution temperature generated samples with 5.06, 7.42 and 8.63 w/o (weight per cent) phosphorus content in the nickel deposit. Immersion gold was deposited at a pH of 5.2 at 85–90 °C from a Schloetter Ormex Gold solution. Deposit height and uniformity was also analysed with the aid of a Tencor Alpha-Step 200 surface profilometer. Differential scanning calorimetry (DSC) was performed to analyse the influence of annealing samples of Ni–P on copper substrates. Triplicate samples of each deposit were scanned in a nitrogen atmosphere from 30 to 400 °C at a rate of 20 °C/min in a Perkin Elmer Pyris 1 DSC. The sample weight was approximately 1.2 mg with the exception of the deposit with 5.06 w/o phosphorus content where 5 mg sample weights were used to improve the signal. The calibration of the instrument was checked with a traceable Indium standard. Powder X-ray diffraction (PXRD) patterns of samples were obtained on a Philips PW 3710 MPD apparatus using Cu Kα [wavelength = 1.5418×10^{-10} m] with a scan rate of 4.2°/min (10–80°) and 2.33°/min (3.15–15°). Samples were prepared for PXRD by deposition on palladium activated (30 s dip in 5.6 mmol solution of $PdCl_2$ acidified with 1 ml of concentrated hydrochloric acid) aluminium on silicon. The poorly adhered electroless nickel film was

removed from the substrate and ground in a mortar and pestle to a fine powder for XRD measurements). Heat treatment of the deposited samples was performed in a nitrogen purged (with oxygen content of < 5 ppm) Solder Reflow Oven (SRO 702) by ATV Technology Inc. at temperatures ranging from 200 to 400 °C for 1 h.

3. Results and discussion

Differential scanning calorimetry (DSC) was used to obtain information on phase changes occurring in the as-plated Ni–P alloys. The crystallisation temperatures of electroless Ni–P deposits with P content in the range 5.06–8.63 w/o (weight per cent) were recorded. The DSC plots of Fig. 1 for a Ni–P deposit with 5.06 w/o phosphorus reveal the appearance of two exotherms with maxima at 244 and 371 °C indicating that the crystallisation process occurs in two steps. That onset of crystallisation in two steps has been attributed [7] to primary crystallisation of nickel in metastable equilibrium with amorphous Ni–P at the lower temperature, in this case 244 °C and a polymorphous reaction resulting in crystalline phases of nickel and Ni_3P at a higher temperature, 371 °C. The lower temperature of crystallisation for the first exotherm 244 °C in this study by comparison with 294 °C in Ref. [7] may be the result of a lower phosphorus content in the deposited material. DSC plots for Ni–P deposits with 7.54 and 8.63 w/o phosphorus reveal the appearance of only one exotherm with a

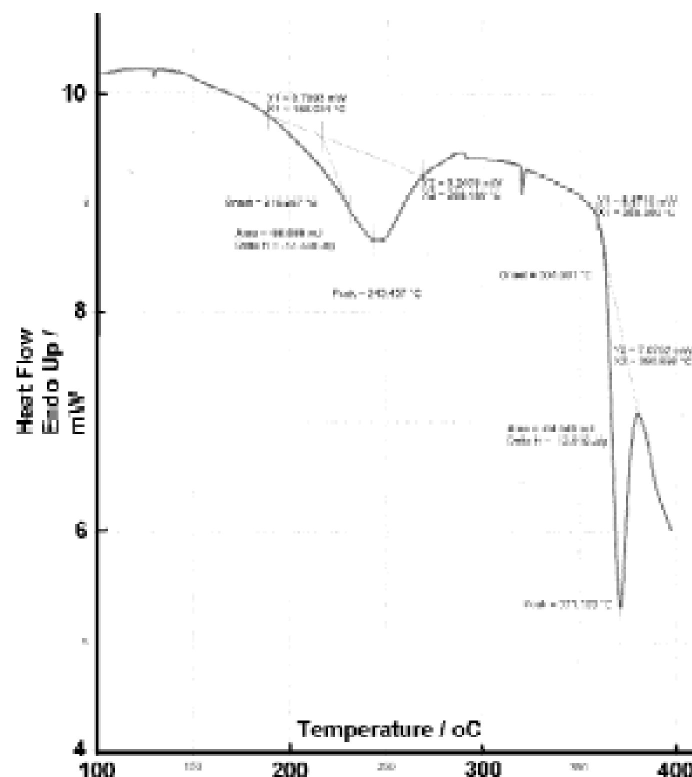

Fig. 1. DSC plot of Ni–P deposits containing 5.06 w/o phosphorus.

maximum at 348 and 363 °C, respectively. Fig. 2 is the DSC plot for Ni–P deposit with 8.63 w/o phosphorus. The absence of an exotherm at a lower temperature supports the observed slow onset of crystallisation in PXRD patterns for heat treated samples with 7.54 and 8.63 w/o phosphorus which will be discussed below.

The as-plated and heat-treated Ni–P deposits were subjected to PXRD analysis. Amorphous halos were obtained with $2\theta = 45^{\circ}$ for each of the three samples with 5.06, 7.54 and 8.63 w/o phosphorus, respectively. The strongest reflection observed was for the sample with lowest P content. As the phosphorus content increased to 8.63 w/o, the reflection becomes less intense, i.e. the degree of crystallinity decreases as phosphorus content increases. An example of the PXRD pattern for the as-plated sample with 7.42 w/o phosphorus is shown in Fig. 3. This figure also depicts the transformation of nickel–phosphorus from amorphous to crystalline, with increasing heat treatment temperature as observed by the sharpening and strengthening of reflections. Rietveld [8] simulation software was used to construct the PXRD patterns of Ni and Ni_3P phases. The reflections observed in Fig. 3 correlate well with the reflections predicted by the simulation software for the increased ratio of crystalline Ni and Ni_3P phases. The phase assignments are indicated in Fig. 3.

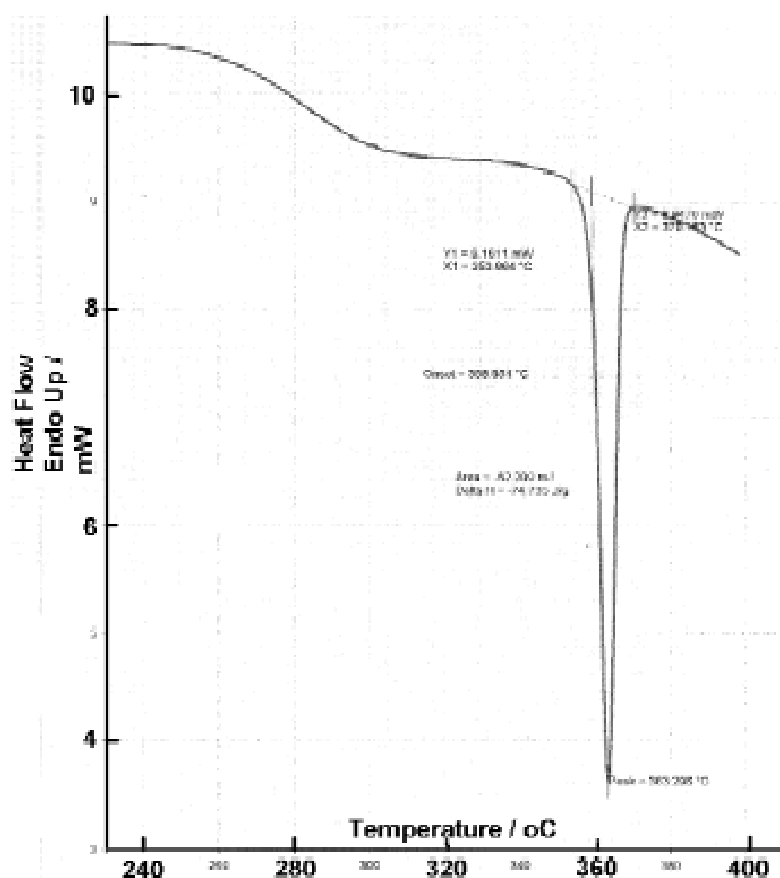

Fig. 2. DSC plot of Ni–P deposits containing 8.63 w/o phosphorus.

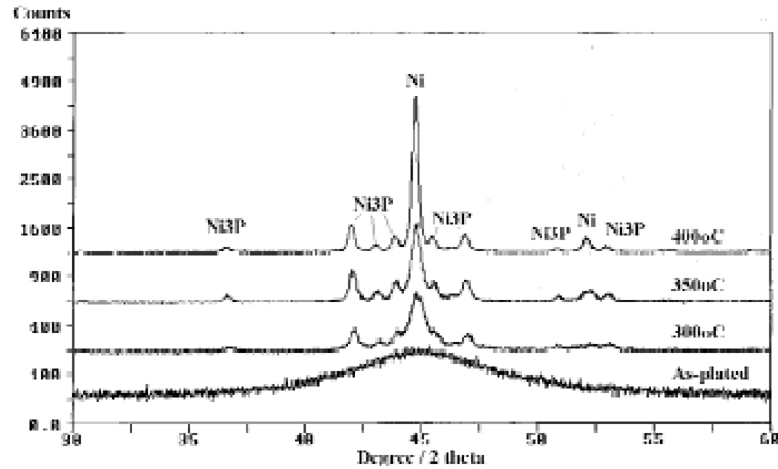

Fig. 3. PXRD of nickel–phosphorus (7.42% P) deposits as-plated and heat treated to 300, 350 and 400 °C. For comparison purposes the diffractograms have been superimposed on the vertical scale.

When X-ray diffraction plots for Ni–P deposits with 5.06, 7.42 and 8.63 w/o phosphorus are qualitatively compared, variations in the rate of crystallisation are observed, such that, an increase in phosphorus content causes a decrease in the rate of crystallisation. PXRD is generally used to qualitatively describe the process of crystallisation. In the present study, crystallisation has been quantified in a manner similar to the measurement of crystallinity in polymers [7,9] where the ratio of integrated crystalline scattering to total scattering of both the crystalline and amorphous phases for deposits at $2\theta = 45^{\circ}$ represents the extent of crystallinity. Using this calculation the amount of transformation of nickel–phosphorus from amorphous to the detectable crystalline Ni and Ni_3P phases with an increase in heat treatment temperature is shown in Table 1. At the lower heat treatment temperature (300 °C), the degree of crystallinity decreases as phosphorus content increases with Ni–P deposits. In general, crystallinity increases to $68 \pm 2\%$ when nickel–phosphorus is heated to about 400 °C. The most dramatic increase is seen for the high phosphorus content (8.63%) sample which had an estimated 8% crystallinity after heat treatment at 300 °C for 1 h in an nitrogen purged environment which increased to 52% at 350 °C. Previous researchers have estimated almost complete

Table 1
Degree of crystallinity of electroless nickel deposit with anneal temperature

Heat treatment temperature	300 °C	350 °C	400 °C
Phosphorus content of Ni–P deposits wt.%	Crystallinity/estimated from PXRD data		
5.06	45%	54%	69%
7.42	32%	53%	68%
8.63	8%	52%	66%

crystallisation of electroless nickel with 12% phosphorus after 2 h at 337 °C in a nitrogen atmosphere [10].

The apparent grain sizes of heat treated nickel–phosphorus alloys with 5.06, 7.42 and 8.63 w/o phosphorus are shown in Table 2. The values represented are based on the Scherrer formula, which makes use of diffraction broadening, as expressed in Eq. (1),

$$t = 0.9\ \lambda / B \cos \theta_{hkl} \tag{1}$$

where t is the apparent thickness of the grain in, λ is the wavelength of the X-ray as defined by Bragg's equation ($\lambda = 2d\ \sin\ \theta$, where d is the spacing between crystal planes) and B is the broadening of the reflection at half its maximum intensity in radians [11]. The data in Table 2 indicates that in general the grain sizes increased with increasing heat treatment temperature and decreased with increasing phosphorus content in the Ni–P alloy. Thus the largest grains were calculated for Ni–P deposit with 5.06 w/o phosphorus and heat treated at 400 °C and the lowest were calculated for Ni–P deposit with 8.63 w/o phosphorus and heat treated at 300 °C. Graham et al. [6] have reported that estimates given by the Scherrer formula are not valid indications of the actual grain size of as-plated alloys with more than 7 w/o phosphorus. Nevertheless, the fact that the estimated grain size for alloys with 5.0 w/o phosphorus was close to the measured value indicates that fine grain size makes a significant contribution to the total breadth of the X-ray reflections from the low-phosphorus alloys.

One of the effects of crystallisation is that hardness increases significantly to a maximum at 400 °C, above which it decreases significantly [12]. The increase in hardness has been attributed to the precipitation of Ni_3P and an increase in the number of lattice defects [7,13]. The maximum microhardness has been observed at 400 °C due to the increased number of nickel grains and hence defects. Above this threshold hardness decreases due, it has been claimed [7], to grain coarsening and a reduction in lattice defects. As already stated, a fine-grained material, i.e. one that has small grains, is harder and stronger than one that is coarse grained, thus from the estimated grain sizes of heat treated samples, Ni–P deposit hardness and strength increases from left to right in Table 3. Thus, based on the mechanism of hardness previously described, from the range of Ni–P deposits studied the hardest alloy contained 8.63 w/o phosphorus.

Cross-sectional SEM analysis provided information on the nickel to wafer interfaces for the as-plated sample and those annealed at 200 and 400 °C. In all samples inspected the nickel deposit

Table 2
Estimated grain size given by Scherrer formula determined from the PXRD data of Ni–P deposits

Phosphorus content of Ni–P deposits wt.%	5.06	7.42	8.63
Heat treatment temperature °C	Estimated grain size in Ni–P alloys/Å		
300	321.6	268.8	223.6
350	358.3	315.2	267.9
400	396.9	357.2	327.4

Table 3
Deposit hardness trend for annealed electroless nickel deposit of different P content based on estimated grain size from PXRD analysis

Phosphorus content of Ni–P deposits wt.%	5.06	5.06	7.42	8.63	5.06	7.42	7.42	8.63	8.63
Anneal temperature °C	400	350	400	400	300	350	300	350	300
Estimated grain size Å	396.9	358.3	357.2	327.4	321.6	315.2	268.8	267.9	223.6
Increasing hardness	--->								

consisted of a void-free deposit with a smooth planar interface between the nickel and copper. The SEM image in Fig. 4 is of a cross-sectioned sample plated for 3 h in the electroless nickel bath, followed by annealing at 400 °C. The area mapped by EDX for elemental distribution at and surrounding the copper to nickel interface is indicated in Fig. 4. The results of the elemental analysis of this section are shown in Fig. 5 which details the distribution of the elements phosphorus, silicon, nickel, copper and titanium at and around the copper to nickel interface from a cross-sectioned sample annealed at 400 °C. The SEM image of the layers for the mapped area is also incorporated in this figure. EDX analysis of samples before and after annealing at 200 °C exhibited no inter-diffusion or

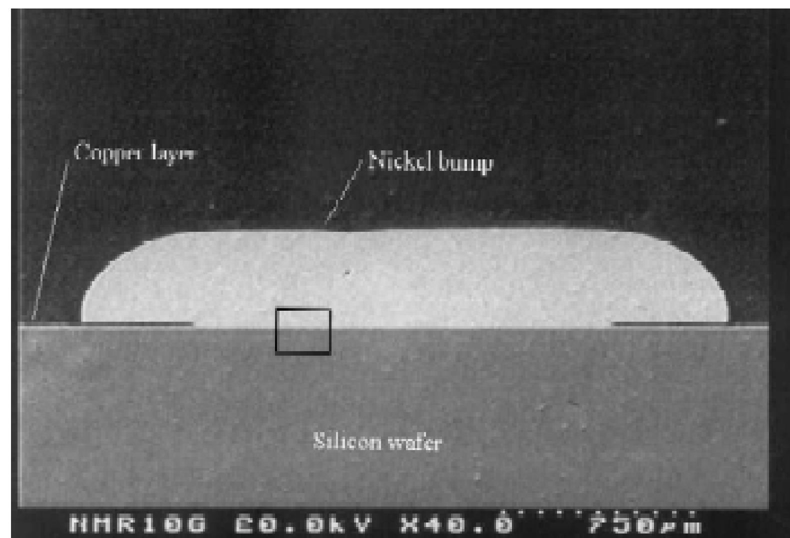

Fig. 4. SEM image of a cross-sectioned nickel plated sample which had been annealed at 400 °C. The area mapped by EDX for elemental analysis (shown in Fig. 5) is indicated.

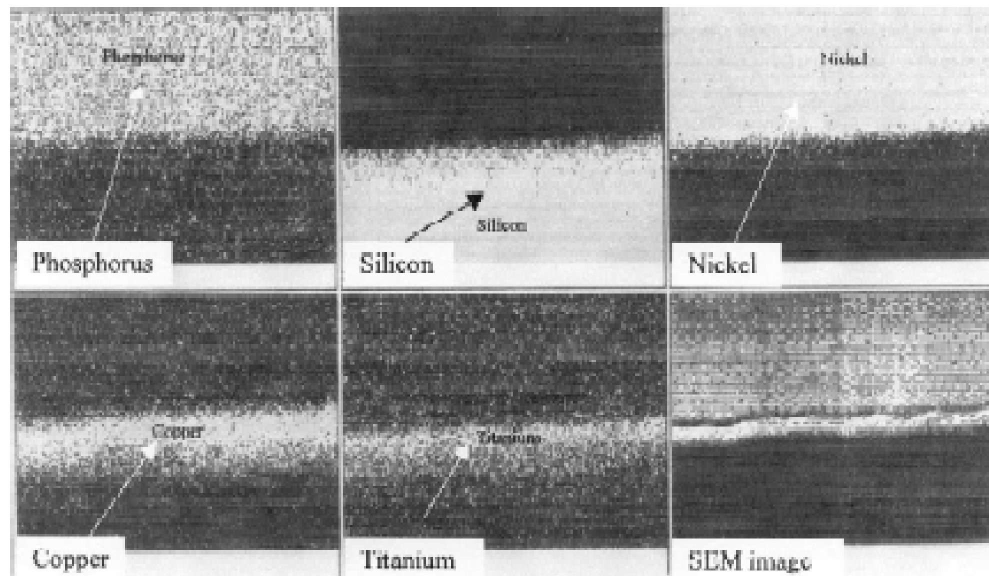

Fig. 5. EDX map of copper to nickel interface for a sample annealed at 400 °C. The top three images from left to right are for phosphorus, silicon and nickel. The second row of images are for copper, titanium and the SEM image of the mapped area.

inter-metallic formation between the interface metallisations. After treatment at 400 °C, the nickel layer appears to have a relatively sharp endpoint by contrast with the copper mapping which would appear to indicate copper movement into the nickel layer. This indicates that the interdiffusion is only permitted with this barrier layer material when the anneal temperature is greater than that required to form Ni_3P crystallites and the majority of the deposit is crystalline as indicated by the PXRD data. It has been claimed that the effectiveness of electroless Ni(P) as a barrier layer depends upon the amorphous nature of the deposit. in which the phosphorus is evenly distributed through the deposit at the grain boundaries obstructing the solid state diffusion path [5].

4. Conclusions

The influence of high temperature processing on the barrier/bonding layer properties of selectively deposited electroless nickel–phosphorus alloys was investigated. The crystallisation behaviour of the deposits with different concentrations of co-deposited phosphorus was examined by DSC and PXRD. Reitveld simulation software was used to verify the presence of Ni and Ni_3P upon heat treatment by assignment of reflections in the experimental data. Crystallisation was quantified in a manner similar to the analysis of crystallisation in polymers. It was shown that the greatest change in crystallisation behaviour was for the deposits with the highest P content once annealed at temperatures above 300 °C. The increase in crystallisation upon heat treatment was found to decrease the effectiveness of the Ni–P as a barrier layer material only for samples annealed at 400 °C. The influence of heat treatment on the grain size and hardness was also investigated for samples with different P content.

Acknowledgements

This work was supported by grant number HE-1999-262 from the Enterprise Ireland Applied Research Grant Scheme.

References

[1] E. Zakel, H. Reichl, Flip chip assembly using gold, gold–tin and nickel–gold metallurgy, in: J.H. Lau (Ed.), Flip Chip Technologies, McGraw Hill Company Inc, 1995, pp. 415–484.
[2] G. Milad, R. Mayes, Electroless nickel/immersion gold finishes for application to surface mount technology: A regenerative approach, Metal Finish. 96 (1998) 42–46.
[3] K.L. Lin, J.W. Chen, Wave soldering bumping process incorporating electroless nickel UBM, IEEE Trans. Compon. Packag. Technol. 23 (2000) 143–150.
[4] NMRC unpublished results.
[5] E.J. O'Sullivan, A.G. Schrott, M. Paunovic, C.J. Sambucetti, J.R. Marino, P.J. Bailey, S. Kaja, K.W. Semkow, Electrolessly deposited diffusion barriers for microelectronics, IBM J. Res. Develop. 42 (1998) 607–620.
[6] A.H. Graham, R.W. Lindsey, H.J. Read, The structure and mechanical properties of electroless nickel, J. Electrochem. Soc. 112 (1965) 401–413.
[7] P.R. Krishnamoorthy, B.H. Narayan, T.V. Ramakrishna, M. Shekhar Kumar, Properties of electroless nickel–phosphorus deposits after crystallisation, Metal Finish., November, 1992.
[8] H.M.A. Rietveld, A profile refinement method for nuclear and magnetic structures, J. Appl. Crystallogr. 2 (1969) 65.
[9] J.F. Rabek, Experimental Methods in Polymer Chemistry, John Wiley & Sons, New York, 1980.
[10] H. Li, H. Chen, S. Dong, J. Yang, J. Deng, Study on the crystallization process of Ni–P amorphous alloy, Appl. Surf. Sci. 125 (1998) 115–119.
[11] C.S. Barrett, Structures of Metals, McGraw–Hill, New York, 1970.
[12] Canning, The Canning Handbook, Surface Finishing Technology, E&F.N. Spon Ltd., London–New York, 1989.
[13] K.L. Lin, P.J. Lai, The crystallization of the electroless Ni–P deposit, J. Electrochem. Soc. 136 (1989) 3803–3808.